JOURNAL OF MATERIALS SCIENCE **40** (2005) 655–662

# Rod milling and thermal annealing of graphite: Passing the equilibrium barrier

D. E. SMEULDERS, A. S. MILEV, G. S. KAMALI KANNANGARA, M. A. WILSON*
*College of Science Technology and Environment, University of Western Sydney, Locked Bag 1797, Penrith South DC, NSW 1797, Australia*
*E-mail: ma.wilson@uws.edu.au*

The change in graphitic carbon structure induced by mechanical milling has been monitored by Raman spectroscopy, transmission electron microscopy (TEM) and X-ray diffraction. It is well known that progressive rod milling of graphite results in an increase in structural disorder. Here, it has been found that a milling time of around 80 h is crucial in producing maximum nanocrystallite formation and this affects the nature of the products formed before or after annealing. At about 80 h equilibrium forms and no further production of nanocrystallites is possible although if additional energy is added amorphous carbon begins to form. Annealing produces different nanographitic carbons depending on the milling conditions because the material may be milled to an equilibrium concentration of nanocrystallites or less, or with additional energy transformed further past equilibrium to new product. Linear morphological structures and trace amounts of carbon nanotubes were found on milling for 80 h and annealing, but concentric layers of carbons were observed in samples milled as long as 240 h. 

## 1. Introduction

Mechanical processing such as ball milling of powders has been studied extensively in recent years with the growing interest in nanocrystalline materials and their unusual properties [1–10]. Zhou *et al*. [4] proposed that milling involved breaking down the graphite into small crystallites, the introduction of defects into the crystallites and then amorphization. However the process is somewhat more complex since Huang *et al*. [11] and Chen *et al*. [12] have recently reported producing nanoarches or curved carbon structures and closed-shell carbon nanostructures such as carbon onions by ball milling graphite. Both Huang *et al*. [11] and Chen *et al*. [12] attribute the formation of closed-shelled or curved carbon structures to the bending of the $sp^2$ sheets under the heavy mechanical deformation of milling. Moreover, Chen *et al*. [13–16] and Chadderton and Chen [17] produced disordered and nanoporous carbon powder by ball milling hexagonal graphite, but upon subsequent thermal annealing they observed that multiwalled carbon nanotubes [18] were formed. They attributed the formation process to be a low temperature, solid-state crystal growth mechanism from what must be an appropriate precursor. Iron was present as a milling contaminant, and the iron might have assisted the formation of nanotubes by causing catalytic growth.

This paper builds upon other work performed by our research group examining the change in the level of disorder of graphite during ball milling in the presence of cobalt and rod milling with yttrium [19, 20], and also the catalytic effect of cobalt in the formation of single walled nanotubes during plasma arcing of carbon [21]. Structural information is obtained by characterizing rod milled and annealed samples by laser Raman spectroscopy, transmission electron microscopy (TEM), and X-ray diffraction (XRD) spectroscopy. Rod milling is generally known to impact more energy on crystallites in a miller of the same volume because of greater surface contact and energy transfer [22] and provides a useful alternative methodology for transforming energy to graphitic lattices than ball milling.

## 2. Experimental

### 2.1. Rod milling and thermal annealing

Tables I and II list rod milling conditions. Hexagonal graphite [4], (particle size $\leq$0.1 mm) was loaded into individual stainless steel mills containing eight hardened stainless steel rods in the presence and absence of 0% and 1% cobalt (0.4 g, Sigma Aldrich—100 mesh, 99.9% purity) as a catalytic agent. Milling was performed at room temperature in an inert nitrogen atmosphere at a pressure of 2 atmospheres. The carbon material was milled at 50 rpm for periods of 40, 60, 80, 120, 180, and 240 h.

After each rod-milling experiment, the milled carbon samples were sub-sampled and stored in a nitrogen environment prior to annealing. Each milled sample was loaded into a ceramic furnace boat and placed inside a 1-inch diameter alumina tube for individual annealing

*Author to whom all correspondence should be addressed.

TABLE I Rod milling conditions

| | |
|---|---|
| Mill | |
| Diameter (cm) | 10.2 |
| Length (cm) | 10.0 |
| Volume ($cm^3$) | 817.1 |
| Speed (rpm) | 50 |
| Rod | |
| Diameter (cm) | 1.9 |
| Length (cm) | 9.4 |
| Weight (g) | 216.7 |
| Density (g $cm^{-3}$) | 8.13 |
| Rods filling, fraction of mill volume | 0.26 |
| Rods per mill | 8 |
| Rod to powder weight ratio | |
| 0% Cobalt | 433:1 |
| 1% Cobalt | 429:1 |

TABLE II Rod milling samples

| Contains | Milling time (h) |
|---|---|
| Graphite | 0 |
| Graphite | 40 |
| Graphite | 60 |
| Graphite | 80 |
| Graphite | 120 |
| Graphite | 180 |
| Graphite | 240 |
| Graphite + 1% (w/w) Cobalt | 40 |
| Graphite + 1% (w/w) Cobalt | 60 |
| Graphite + 1% (w/w) Cobalt | 80 |
| Graphite + 1% (w/w) Cobalt | 120 |
| Graphite + 1% (w/w) Cobalt | 180 |
| Graphite + 1% (w/w) Cobalt | 240 |

at 1400°C in a tube furnace. Annealing experiments were performed under an atmosphere of ultra high purity argon, which was passed through the alumina tube at a flow rate of at least 30 mL/min. A length of narrow diameter Teflon tubing was connected to the outlet of the alumina tube to minimize oxygen diffusion back into the furnace. Annealing of each sample took approximately 15 h as the furnace required 3 h to reach 600°C, and then another 6 h to reach the annealing temperature of 1400°C. Each sample was annealed at 1400°C for a period of 6 h. At the completion of annealing the power to the furnace was disconnected and the sample and tube were allowed to cool overnight. The inert argon flow was maintained over the sample during cooling. Samples so prepared were analysed by a variety of techniques as described below.

### 2.2. Laser Raman spectroscopy

The Raman spectra were acquired on a Renishaw Raman Microprobe Laser Raman Spectrometer with the collection optics based on a Leica DMLM microscope. A refractive glass 50X objective lens was used to focus the laser onto a 2 $\mu$m spot to collect the backscattered radiation. The 514.5 nm line of a 5W $Ar^+$ laser (Spectra-Physics Stabilite 2017 laser) was used to excite the sample. Surface laser powers of 1.0–1.5 mW were used because the milled and annealed graphite samples were found to burn under higher energies. Milled and annealed graphite samples were deposited on clean aluminum microscope slides and irradiated with the laser to obtain each spectrum. Ten scans with an accumulation time of 30 s were used to collect the spectrum over the scan range from 1000–1800 $cm^{-1}$.

### 2.3. X-ray diffraction (XRD) spectroscopy

A Philips PW1729 X-ray generator with a copper X-ray tube operating at a power of 30 mA and 40 kV was used. Samples were dispersed in acetone and a few drops of the liquid were pipetted onto a silicon sample holder. The acetone was allowed to evaporate before the sample holder was inserted into the camera. A diffractogram was collected for each sample between 10.00–100.00°$2\theta$ with steps of 0.02 °$2\theta$ and a count time of 1 s per step.

### 2.4. Transmission electron microscopy (TEM)

High Resolution TEM was obtained on a JEOL 3000F Field Emission Gun (FEG) operating at 300 kV, or a Philips Biofilter operating at 120 kV. Care was taken not to produce carbon nanotubes in these products by electron irradiation by avoiding holy carbon support films [23].

## 3. Results and discussion

### 3.1. Raman spectroscopy

The first order spectrum of a graphite single (or infinite) crystal exhibits a single line at 1580 $cm^{-1}$, which is designated as the G band (*graphite*) [24–26]. Structural disorder results in broadening of the sharp G band and the appearance of a second line at ∼1360 $cm^{-1}$, designated as the D band (*defects*). The D band is assigned to a breathing mode forbidden in the perfect infinite graphite sheet, becoming active only with disorder [24–26]. A D′ band at ∼1620 $cm^{-1}$ occurs (ignored in the treatment here) only in disordered carbons and imperfect graphite and is responsible for what is an apparent up-shift of the G band. The width and relative intensities of D and G lines vary with structural evolution and may be used to characterize carbon materials.

The ratio of band intensities $I_D/(I_D + I_G)$, expressed as a percentage, is most frequently used as a disorder parameter, and the G band full width half maximum (FWHM) is also used.

Table III and Fig. 1 shows Raman data and plots for 1% cobalt and graphite, and graphite samples respectively that have been milled for 40 to 240 h. Elsewhere [19, 20] under ball rather than rod milling conditions we have studied the effects of 1 and 10% cobalt. It is necessary here to repeat the 1% cobalt work with rod milling under the same conditions as pure graphite to investigate the effect of 1% cobalt. Fig. 1 clearly shows that milling increases the $I_D/(I_D + I_G)$ ratio of the carbon up to a maximum of 49.9% after 80 h of milling. Fig. 1 shows that both the samples containing 1% cobalt and graphite, and pure graphite, exhibited the same trends for disorder with milling time (data is superimposed at ≤80 h) indicating that the cobalt did not dramatically change the milling action when present as an additive at 1% concentration. Further milling beyond 80 h leads

TABLE III Raman spectroscopy results for rod milled samples of graphite, and 1% cobalt and graphite

| Milling time (h) | Contains | G FWHM ($cm^{-1}$) | D FWHM ($cm^{-1}$) | D/G (from area) | $I_D/(I_D + I_G)$ (%) | $I_D/I_G$ |
|---|---|---|---|---|---|---|
| Unmilled graphite | Carbon | 19.0 | 44.3 | 0.20 | 12.31 | 0.14 |
| 40 | Carbon | 56.3 | 88.0 | 1.07 | 42.55 | 0.74 |
| 60 | Carbon | 81.0 | 100.0 | 1.36 | 47.08 | 0.89 |
| 80 | Carbon | 117.3 | 123.7 | 1.40 | 49.89 | 1.00 |
| 120 | Carbon | 178.0 | 181.0 | 1.27 | 49.37 | 0.98 |
| 180 | Carbon | 188.0 | 204.0 | 1.15 | 47.97 | 0.92 |
| 240 | Carbon | 187.0 | 212.0 | 1.10 | 46.70 | 0.88 |
| 40 | Carbon + 1% Cobalt | 58.7 | 92.7 | 1.12 | 41.92 | 0.72 |
| 60 | Carbon + 1% Cobalt | 99.0 | 118.0 | 1.42 | 48.81 | 0.95 |
| 80 | Carbon + 1% Cobalt | 129.3 | 124.3 | 1.35 | 50.30 | 1.01 |
| 120 | Carbon + 1% Cobalt | 182.0 | 183.0 | 1.33 | 49.61 | 0.98 |
| 180 | Carbon + 1% Cobalt | 183.0 | 198.0 | 1.14 | 48.02 | 0.92 |
| 240 | Carbon + 1% Cobalt | 189.0 | 217.0 | 1.08 | 46.61 | 0.87 |

G-G band (Graphite), D-D band (Defects) FWHM-full width at half maximum, 1-ban intensity for band D or G.

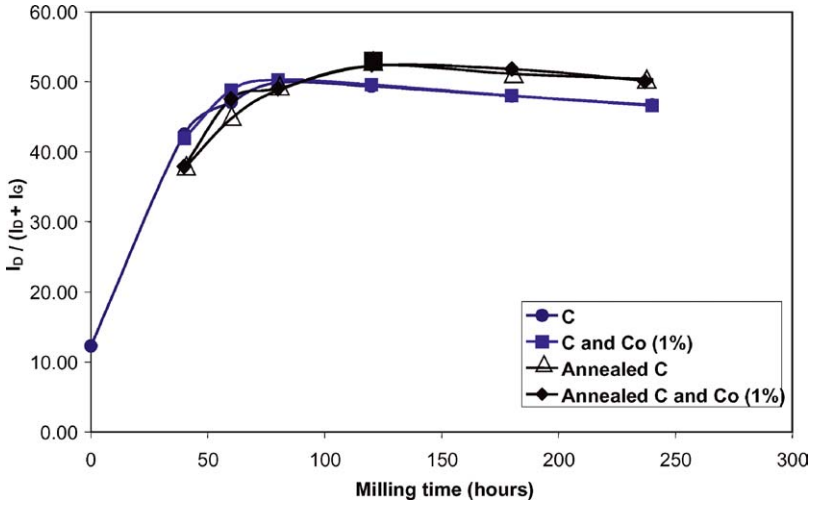


*Figure 1* Plot of graphite, and 1% cobalt and graphite samples that have undergone ball milling from 0 to 240 h—before and after annealing, against the structural disorder $I_D/(I_D + I_G)$ ratio.

to a gradual decrease in the $I_D/(I_D + I_G)$ ratio to 46.7% after 240 h, which is possibly just outside experimental error (about 2%). We did not observe this effect with ball milling in the presence of cobalt or rod milling with yttrium [20].

The decrease in $I_D/(I_D + I_G)$ and hence the increase in order should not necessarily be due to realignment of graphitic planes, rather it may be that a different type of material is produced which has a different Raman response. Indeed, Fig. 2 shows that at long milling times (>80 h), the D and G bands begin to merge to form a single broad asymmetrical band associated with amorphous carbon, indicating the loss of three-dimensional ordering in the graphite

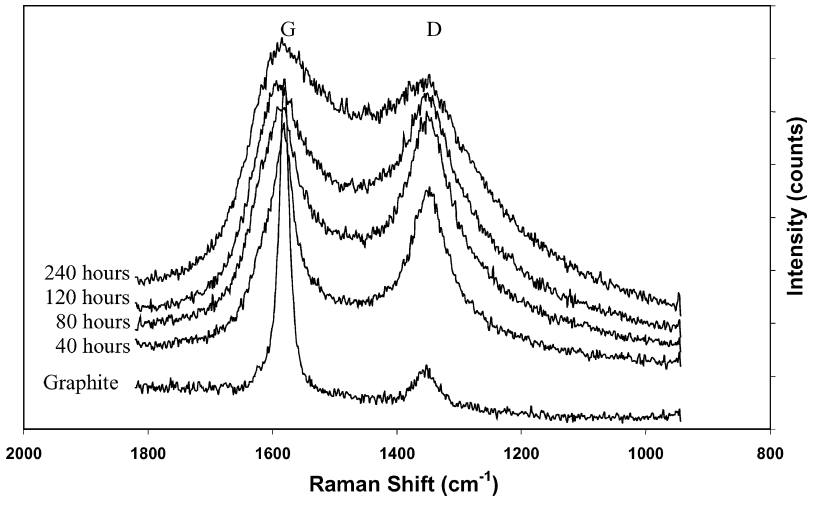


*Figure 2* Stack plot of Raman spectra for graphite milled for 0, 40, 80, 120 and 240 h showing the change in size and shape of the D and G bands.

TABLE IV Raman spectroscopy results for rod milled and subsequently annealed samples of graphite, and 1% cobalt and graphite

| Milling time (h) | Contains | G FWHM ($cm^{-1}$) | D FWHM ($cm^{-1}$) | D/G (from area) | $I_D/(I_D + I_G)$ (%) | $I_D/I_G$ |
|---|---|---|---|---|---|---|
| 40 | Carbon | 35.3 | 57.0 | 0.88 | 37.65 | 0.60 |
| 60 | Carbon | 53.3 | 64.3 | 1.04 | 44.71 | 0.81 |
| 80 | Carbon | 63.0 | 65.7 | 1.15 | 48.75 | 0.95 |
| 120 | Carbon | 72.0 | 69.7 | 1.26 | 52.32 | 1.10 |
| 180 | Carbon | 74.3 | 80.7 | 1.30 | 51.15 | 1.05 |
| 240 | Carbon | 78.0 | 86.0 | 1.25 | 50.36 | 1.01 |
| 40 | Carbon + 1% Cobalt | 36.3 | 57.0 | 0.84 | 37.90 | 0.61 |
| 60 | Carbon + 1% Cobalt | 62.3 | 66.3 | 1.13 | 47.56 | 0.91 |
| 80 | Carbon + 1% Cobalt | 66.0 | 70.0 | 1.18 | 49.04 | 0.96 |
| 120 | Carbon + 1% Cobalt | 74.7 | 73.7 | 1.28 | 52.27 | 1.10 |
| 180 | Carbon + 1% Cobalt | 75.7 | 78.7 | 1.32 | 51.84 | 1.08 |
| 240 | Carbon + 1% Cobalt | 79.7 | 85.7 | 1.30 | 50.08 | 1.00 |

during extended milling. Amorphous carbon exhibits a single broad asymmetrical band in the region of 1000–1800 $cm^{-1}$, centered at 1500 $cm^{-1}$. Thus the results suggest the nanocrystallites of carbon restructure to amorphous carbon at >80 h and that the material is different in structure from that formed by ball milling. Amorphous carbon is probably in $sp^2$ hybridisation without discretely ordered aromatic lamellae.

Table IV and Fig. 1 also shows the $I_D/(I_D + I_G)$ ratios for the graphite, and graphite and cobalt samples after annealing, and it is clear that annealing produced structural change in the milled material. For the samples milled for 80 h annealing decreased the $I_D/(I_D+I_G)$ ratio and the amount of disorder in the samples. For example, the graphite sample milled for 40 h had a decrease in the $I_D/(I_D + I_G)$ ratio from 42.6% to 37.7% due to annealing. For longer milling times (>80 h) annealing increased the $I_D/(I_D+I_G)$ ratios relative to the material that was only milled. For example, the graphite sample milled for 180 h showed an increase in the $I_D/(I_D+I_G)$ ratio from about 47.9 to 51.1% due to annealing.

Thus less than 60 h or so when the nanocrystalline units of graphite are present they can be converted back into an ordered structure by annealing, but once amorphous carbon is formed the same degree of order cannot be attained.

This result is quite different to that obtained in ball milling experiments, where annealed samples are always more ordered that unannealed samples. They further illustrate that the disordered phase formed by rod milling at greater than 80 h milling time is unable to transform back to a more ordered phase like the material formed by ball milling.

## 3.2. X-ray diffraction (XRD) analysis

The X-ray diffractograms for typical samples (0 and 80 h) are shown in Fig. 3. The patterns reveal that changes in the shape, intensity and breadth of the peaks occur as a function of milling time. Whereas X-ray diffraction analysis of the graphite starting material revealed strong (*002*), (*004*), and (*006*) diffraction peaks, as well as minor peaks for (*100*), (*101*), (*103*), (*110*) and (*112*) reflections, Fig. 3 shows that with milling the main graphite reflection, (*002*), becomes less intense and broadens, while the graphite reflections (*004*) and (*006*) disappear. Broadening of the $C_{(002)}$ reflection is attributed to increasing interlayer disorder within the graphitic structure. It is noteworthy to mention that reflections due to iron and iron carbide phases emerged with increasing milling time, which can be attributed to the abrasion of the stainless steel rods and mill. Iron and iron carbide contaminant peaks were observed at 45°, 43.6°, 50.7°, 74.7° and 90.7° and are marked with the * symbol. The contaminant peaks are barely discernable after 80 h of milling, however

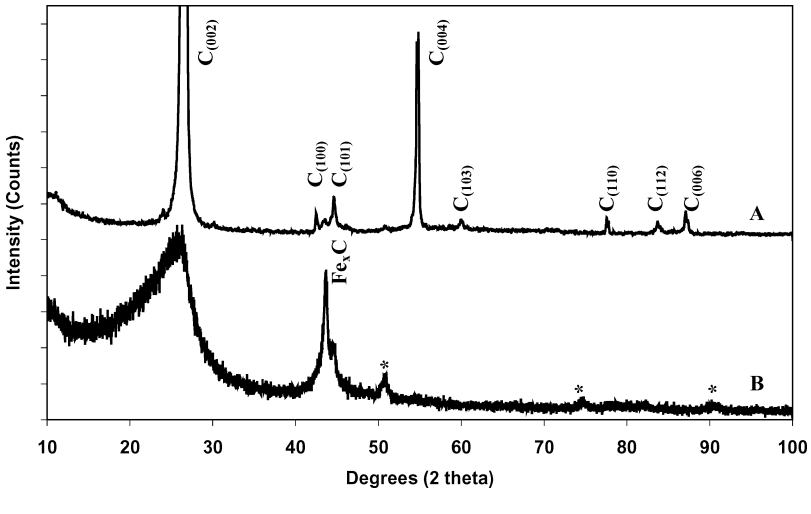


*Figure 3* X-ray diffractograms for rod milled graphite samples. (A) Graphite milled for 0 h. (B) Graphite milled for 80 h.

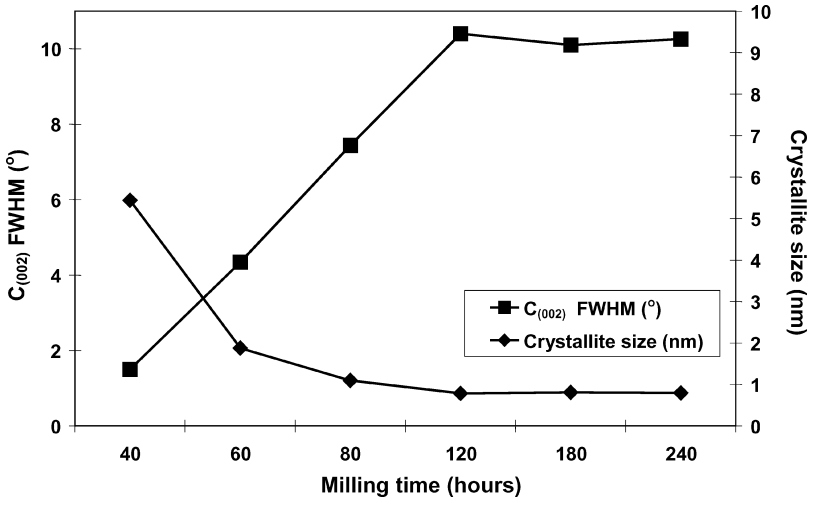


*Figure 4* Plot of the FWHM (degrees) of the $C_{(002)}$ reflection and the crystallite size ($L_c$) in nm, for the 1% cobalt and graphite samples milled for between 40 and 240 h without annealing.

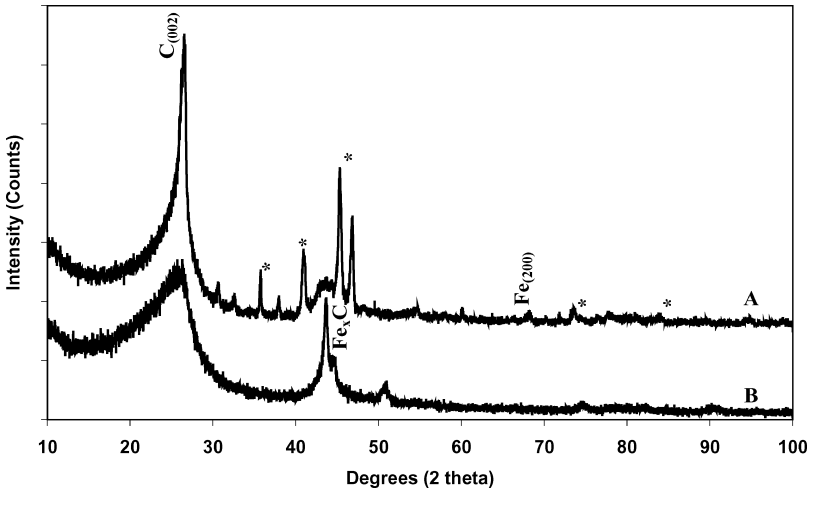


*Figure 5* X-ray diffractograms for rod milled graphite samples before and after annealing. (A) Graphite milled for 80 h and subsequently annealed. (B) Graphite milled for 80 h.

these peaks become better resolved with longer milling times.

Fig. 4 shows a plot of the FWHM of the $C_{(002)}$ reflection for the 1% cobalt and graphite samples rod milled for up to 240 h without annealing. The FWHM of the $C_{(002)}$ reflection can be directly related to the crystallite size $L_c$ [26–29], and the changes in crystallite size during milling are also shown in Fig. 4. A significant reduction in crystallite size and an increase in FWHM values occur during milling. Clearly these results also suggest that a nanocrystalline phase no longer exists in any concentration above 80 h.

Fig. 5 shows the diffractograms obtained for a graphite sample that had been milled for 80 h (Fig. 5B) and subsequently annealed (Fig. 5A). The diffractograms showed large changes as a result of annealing. The (*002*) diffraction peak went from being a broad hump in the milled material to sharp and intense in the annealed samples, indicating significant structural change during annealing due to the growth of two-dimensional graphitic layers. In addition, several of the reflections seen in the milled material disappeared, and numerous new reflections appeared in the annealed material. The strong reflections in the milled material at 43.6°, 50.7, 74.7°, and 90.7° all disappeared during annealing. New reflections at 35.7°, 40.7°, 45.4°, 66.1°, 73.5°, and 83.8° appeared during annealing. These new reflections are shown in Fig. 5 with the symbol *. None of these new peaks had been observed in the material that had only been milled, and they were also not observed in the original graphite. The peak at 66.1° has been assigned to the $Fe_{(200)}$ reflection, the other new reflections observed by XRD come from the different forms of carbon produced during annealing in addition to the peaks derived from the phase transitions of metal and metal carbides at the high temperatures.

The presence of cobalt at 1% did not produce any additional reflections in the X-ray diffractograms of either the milled or annealed samples. Essentially the diffractograms were identical for the samples with and without cobalt. A Plot of the FWHM (degrees) of the $C_{(002)}$ reflection and the crystallite size ($L_c$) in nm, for the 1% cobalt and graphite samples milled for between 80 and 240 h with annealing (Fig. 6) shows like the

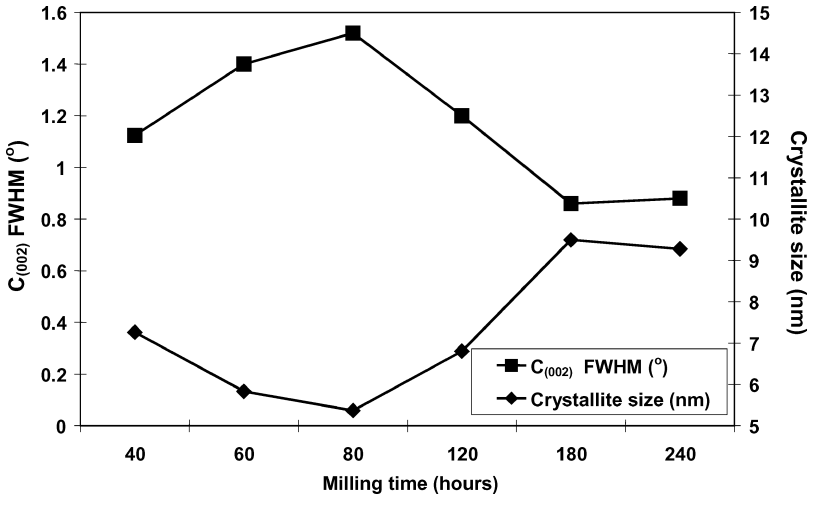


*Figure 6* Plot of the FWHM (degrees) of the $C_{(002)}$ reflection and the crystallite size ($L_c$) in nm, for the 1% cobalt and graphite samples milled for between 40 and 240 h with annealing.

Raman data that after 80 h a different annealed product is formed. Before 80 h the microcrystallites affect the ordering of the annealed product. The annealed product reflects how far the material has been transformed from graphite, as illustrated elsewhere for ball milling [19]. However once the amorphous product is formed there is a change in the nature of the annealed product.

## 4. Transmission electron microscopy

TEM micrographs of milled material before and after 80 h did not reveal any information on a transformation of product after around 80 h, only the gradual loss of crystallites of graphite up to 80 h. The equivalent results after annealing were more interesting. Trace amounts of carbon nanotubes were found on milling for 80 h but in general the TEMs showed linear morphological structures (illustrated Fig. 7A). Concentric layers of carbons were observed in milled samples as long as 240 h (Fig. 7B) showing that annealing of amorphous carbon does reform different nanostructures as suggested by XRD and Raman. However it is unclear whether these are joined at the ends to form concentric structures with five membered rings accounting for the curvature (sometimes called buckyonions).

## 5. Mechanism

It is clear that carbon becomes more amorphous with extended milling time. This is not new. Cobalt, when present at 1% w/w of the graphite did not disrupt the rod milling of the graphite unlike experiments previously reported with 10% cobalt or yttrium. The results indicate that this process is over at 80hr and but further milling disrupts the formation of nanocrystallites and produces amorphous carbon. Under ball milling conditions at least in the reactors discussed here, the product is microcrystalline, but in rod milling it progresses further to a new phase, which often described as amorphous, but actually because it has reformed and is not microcrystalline has more order, albeit of a different form. This new phase production can be influenced by metals since in the presence of yttrium it is not seen [20]. During nanocrystallite formation, the system will be driven to minimise its free energy by the elimination of dangling surface bonds. As the nanocrystallites become smaller and smaller then there will be an increasing desire to react. The 80 h point represents the time when the chemical potential of recombination is in equilibrium with the chemical potential of bond destruction. The actual product formed will depend therefore on the thermodynamic stability of the carbon clusters so formed. This is graphitic or other $sp^2$ hybridised material depending on cluster size, and hence it is unlikely that carbon nanotubes might form.

Raman spectroscopy and X-ray diffraction indicated a dramatic reduction in the amount of disorder in the milled material when it was annealed at 1400°C. However the effects were milling time dependent and differ for rod milling and ball milling. Carbon nanotubes were not significantly observed under any of the conditions although there was trace evidence for some extremely small amounts at 80 h milling times followed by annealing which is possible significant since this is the maximum nanocrystallite time. While it may be possible to form such structures by annealing, it is unlikely since in effect annealing just shifts the graphite or amorphorus material into a more ordered or disordered material respectively. Rather the methodology necessary for nanotube formation would be to catalytically speed up the reaction to a non equilibrium product, or prestablise nanocrystallite structures so that they may form carbons of even smaller units down to the five membered or even single atom precursors observed in plasma arcing experiments.

The process is not improved by yttrium or cobalt catalyst because these are not implicated in producing a non equilibrium product. It seems probable that the key to producing large quantities of carbon nanotubes by milling is effectively to reproduce the carbon arcing experiment in the solid state. In short that means isolating carbon clusters or atoms as much as possible by a dilutent. Indeed this has been the success in forming useful new nanostructured materials from inorganic sources [30]. Further work is being directed to this process.

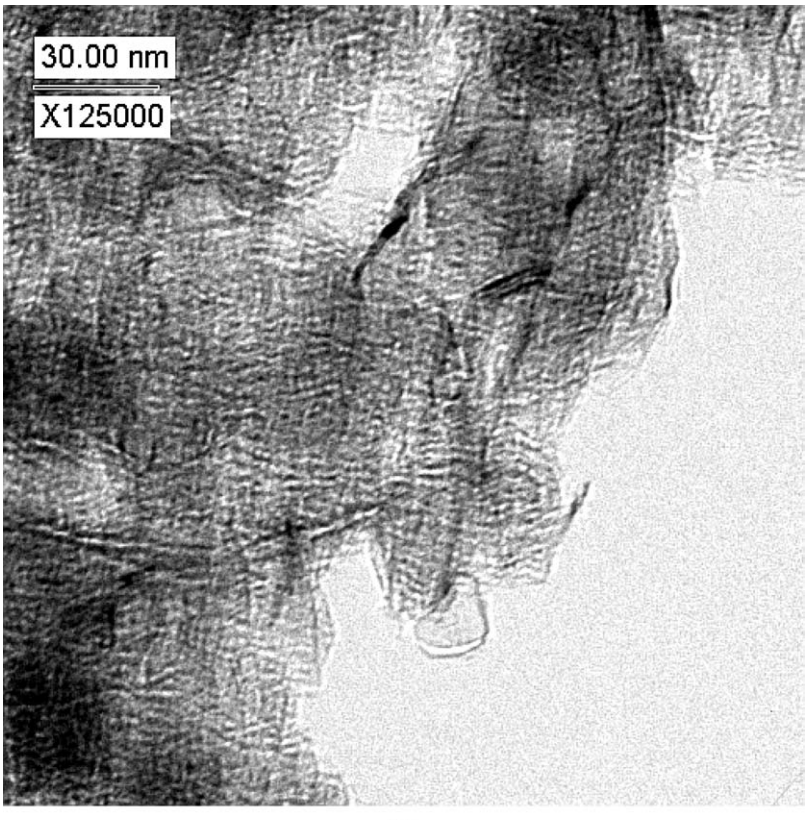


(A)

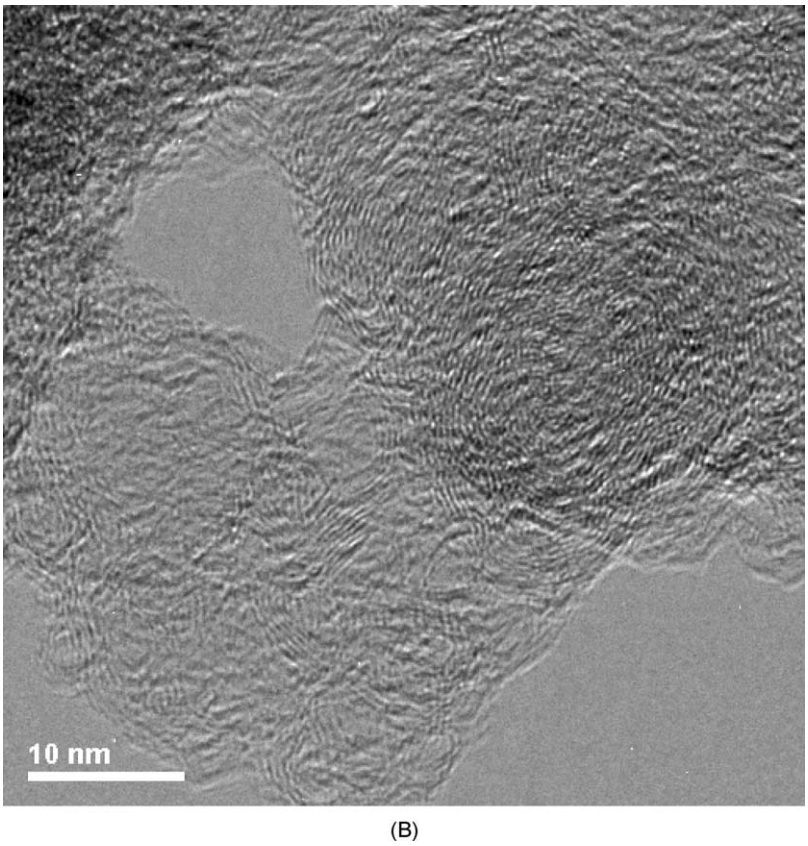


(B)

*Figure 7* TEM of material obtained (A) 80 h milling with 1% Co annealed for 6 h (B) 240 h milling with 1% Co and annealed for 6 h.

## 6. Conclusions

1. Extended rod milling of graphite in the presence in the presence and absence of 1% cobalt w/w introduces structural defects into the graphitic structure, which is clearly shown by Raman spectroscopy and XRD analyses. At about 80 h the process is complete and equilibrium forms. No further production of nanocrystallites is possible. However in systems with additional energy equilibrium can be disturbed and amorphous carbon begins to form.

2. Annealing produces different nanographitic carbons depending on the milling conditions because the material may be milled to an equilibrium concentration of nanocrystallites or less, or under rod milling conditions transformed further past equilibrium to new product.

3. Trace amounts of carbon nanotubes were found on milling for 80 h but in general the TEMs showed linear morphological structures. Concentric layers of carbons were observed in milled samples as long as 240 h, showing that annealing of amorphous produces different products different aligned structures.


## Acknowledgements

We would like to thank Dr. Craig Marshall (Macquarie University) for technical advice on milling and analysis, as well as Dr. Stephen Sestak and Dr. Simon George (CSIRO Petroleum) for assistance with annealing experiments.


## References


1. K. NIWASE, T. TANAKA, Y. KAKIMOTO, K. N. ISHIHARA and P. H. SHINGU, *Mater. Trans J.I.M.* **36** (1995) 282.
2. T. D. SHEN, WQ. GE, K. Y. WANG, M. X. QUAN, J. T. WANG and W. D. WEI, *Nanostructed Materials* **7** (1996).
3. J. TANG, W. ZHAO, L. LI, A. U. FALSTER, W. B SIMMONS and W. L. ZHOU, *J. Mater Res* **11** (1996) 733.
4. W. L. ZHOU, Y. IKUHARA, W. ZHAO and J. TANG, *Carbon* **33** (1995) 1177.
5. J. B. ALADEKOMA and R. H. BRAGG, *ibid.* **28** (1990) 897.
6. M. NAKAMIZO, H. HONDA and M. INAGAKI, *ibid.* **16** (1978) 281.
7. T. S. ONG and H. YANG, *ibid.* **38** (2000) 2077.
8. H. HERMANN, T. SCHUBERT, W. GRUNER and N. MATTERN, *Nanostruct. Mater.* **8** (1997) 215.
9. T. FUKUNGA, K. NAGANO, U. MIZUTANI, H. WAKAYAMA and Y. FUKUSHIMA, *J. Non-Cryst. Solids* **232** (1998) 416.
10. N. J. WELHAM and J. S. WILLIAMS, *Carbon* **36** (1998) 1309.
11. J. Y. HUANG, H. YASUDA and H. MORI, *Chem. Phys. Lett.* **303** (1999) 130.
12. Z. H. CHEN, H. S. YANG, G. T. WU, M. WANG, F. M. DENG, X. B. ZHANG, J. C. PENG and W. Z. LI, *J. Crystal Growth* **218** (2000) 57.
13. Y. CHEN, L. T. CHADDERTON, J. S. WILLIAMS and G. J. FITZ, *Mater. Sci. Forum* **343–346** (2000) 63.
14. Y. CHEN, M. J. CONWAY and G. J. FITZ, *Appl. Phys. A* (2002) Online publication: DOI: 10.1007/s00339-002-(1986) 3.
15. Y. CHEN, G. J. FITZ, L. T. CHADDERTON and L. CHAFFRON, *J. Metastable and Nanocrystalline Mater* **2–6** (1999) 375.
16. *Idem.*, *Appl. Phys. Lett.* **74** (1999) 2782.
17. L. T. CHADDERTON and Y. CHEN, *Phys Lett A* **263** (1999) 401.
18. S. IIJIMA, *Nature* **354** (1991) 56.
19. C. P. MARSHALL and M. A. WILSON, *Carbon* **42** (2004) 2179.
20. H. CONNAN, B. REEDY, C. P. MARSHALL and M. A. WILSON, *Energy and Fuels* **18** (2004) 1607.
21. J. KALMAN, C. NORDLUND, H. K. PATNEY, L. A. EVANS and M. A. WILSON, *Carbon* **39** (2001) 137.
22. R. BIRRINGER and H. GLEITER, in "Encylopedia of Materials Science," edited by R. W. Cahn (Pergamon Press, 1988) vol. 1 (Supp.), p. 379.
23. P. J. F. HARRIS, *Carbon* **39** (2001) 909.
24. F. TUINGSTRA and J. L. KOENIG, *J. Chem. Phys.* **53** (1970) 1126.
25. P. LESPADE, R. AL-JISHI and M. S. DRESSELHAUS, *Carbon* **5** (1982) 427.
26. A. CUESTA, P. DHAMELINCOURT, J. LAUREYNS, A. MARTINEZ-ALONSO and J. M. D. TASCON, *ibid.* **32** (1994) 1523.
27. J. DONG, W. C. SHEN, B. F. ZHANG, F. Y. KANG, X. LIU, J. L. GU, D. S. LI, X. F. HU and N. P. CHEN, *J. Phys. Chem. Solids* **62** (2001) 2047.
28. B. BOKHONOV and M. KORCHAGIN, *J. Alloys and Compounds* **333** (2002) 308.
29. M. ENDO, C. KIM, T. KARAKI, T. KASA, M. J. MATTHEWS, S. D. M. BROWN, M. S. DRESSELHAUS, T. TAMAKI and T. NISHIMURA, *Carbon* **6** (1998) 1633.
30. M. A. WILSON, G. S. K. KANNANGARA, G. SMITH, M. SIMMONS and B. RAGUSE (Nanotechnology Chapman Hall, Boca Raton USA, 2002) p. 75.



*Received 2 March*
*and accepted 20 September 2004*